Multifaceted Ultrafast Intramolecular Charge Transfer Dynamics of 4-(Dimethylamino)benzonitrile (DMABN)

ARTICLE *in* THE JOURNAL OF PHYSICAL CHEMISTRY A · DECEMBER 2012

Impact Factor: 2.69 · DOI: 10.1021/jp310842z · Source: PubMed

3 AUTHORS, INCLUDING:

Taiha Joo
Pohang University of Science and Technology
131 PUBLICATIONS **4,035** CITATIONS

THE JOURNAL OF PHYSICAL CHEMISTRY A

Article

pubs.acs.org/JPCA

Multifaceted Ultrafast Intramolecular Charge Transfer Dynamics of 4-(Dimethylamino)benzonitrile (DMABN)

Myeongkee Park,[†] Chul Hoon Kim,[‡] and Taiha Joo*[,†]

[†]Department of Chemistry, Pohang University of Science and Technology (POSTECH), Pohang 790-784, Korea

[‡]Max Planck Center for Attosecond Science (MPC-AS), POSTECH, Pohang 790-784, Korea

Supporting Information

ABSTRACT: Intramolecular charge transfer (ICT) of DMABN has been the subject of extensive investigations. Through the measurements of highly time-resolved fluorescence spectra (TRFS) over the whole emission region, we have examined the ICT dynamics of DMABN in acetonitrile free from the solvation dynamics and vibronic relaxation. The ICT dynamics was found to be characterized by a broad range of time scales; nearly instantaneous (<30 fs), 160 fs, and 3.3 ps. TRFS revealed that an ICT state with partially twisted geometry, ICT(P), is formed within a few hundred femtoseconds either directly from the initial photoexcited state or via the locally excited (LE) state. The ICT(P) state undergoes further relaxation along the intramolecular nuclear coordinate to reach the twisted ICT (TICT) state with the time constant of 4.8 ps. A conformational diversity along the rotation of the dimethylamino group was speculated to account for the observed diffusive dynamics.

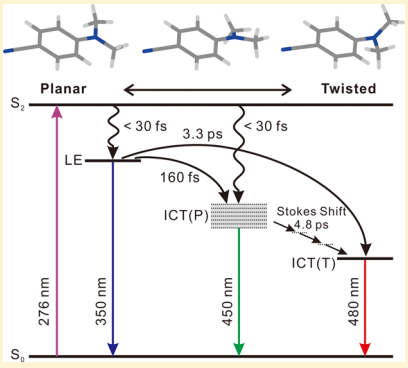

1. INTRODUCTION

4-(Dimethylamino)benzonitrile (DMABN), a benchmark molecule for the experimental and theoretical studies on the intramolecular charge transfer (ICT) reaction, exhibits dual fluorescence from the locally exited (LE) and the intramolecular charge transfer (ICT) states in polar solvents.[1−3] The LE state emits at 350 nm with a small Stokes shift from the absorption band at 290 nm, whereas the ICT state shows extremely large Stokes shift in polar solvents.[4] The ICT emission of DMABN is very sensitive to the solvent polarity, and molecules showing characteristics similar to that of DMABN such as Laurdan (6-lauroyl, 1-2-dimethylamino naphthalene) have been exploited to probe the solvent environment in cell imaging.[5,6]

Although DMABN has a simple molecular structure, nature of the dual emission has not been fully revealed. Dynamics of the ICT reaction and the structure of the ICT state has been the subject of intense discussion for several decades, prompted by the contradictory experimental and theoretical results depending on the techniques to probe the ICT state.[7−22] Early investigations concluded that the ICT state has a twisted conformation between the electron donating dimethylamino group and the phenyl ring, i.e., the twisted ICT (TICT) model, and that the large amplitude rotation of the dimethylamino group is essential for the ICT reaction.[1,3,23] In addition to the TICT model, several other models such as planar ICT (PICT),[24,25] wagged ICT (WICT),[26,27] and rehybridized ICT (RICT)[28,29] have been proposed to describe the structure of the ICT state.

The ICT reactions of DMABN and related compounds have been studied by time-resolved fluorescence (TRF) and transient absorption (TA) methods to resolve the ICT dynamics. Recently, analogues of DMABN with alkyl-substitution or rigidized amino group have been examined by Zachariasse and co-workers, and the results support the PICT model.[30−33] In particular, ultrafast ICT reaction of a planarized analogue of DMABN, 1-tert-butyl-6-cyano-1,2,3,4-tetrahydroquinoline (NTC6),[30,31] and the picosecond X-ray diffraction experiment of 4-(diisopropylamino)benzonitrile[34] substantiated the PICT model. However, Rettig and co-workers have contended that the ICT emission originates from the TICT state, whose energy is lowered by the twist of the amino group. On the basis of the dependences of the ICT rate on the donor group size and solvent viscosity in their femtosecond TRF experiment,[35] large amplitude twisting motion of the donor was proposed to be the rate determining step. A different view on the ICT dynamics was suggested by Lim and co-workers.[36,37] Their femtosecond TRF and TA experiments show different ICT reaction time constants of 3 and 4.1 ps, respectively. This phenomenon was explained by the presence of two different ICT states, a dark TICT and fluorescent ICT states.

Extensive quantum mechanical calculations have been reported to describe the structures of the ICT state and the ICT dynamics. Several calculations reported that the energy of the ICT state is lowered by the twisting or wagging of the amino group in polar solvents, supporting the TICT model.[13,14,23,38−41] A TDDFT calculation by Rappoport and Furche identified an intersection between the LE and ICT states, where the vibronic coupling is strong and the energy barrier for the twisting is small.[42] They also noted that the

Received: November 2, 2012
Revised: December 6, 2012
Published: December 18, 2012

existing ICT models are oversimplified in its complexities. Gómez et al. showed that the PICT concept cannot be excluded in the ICT reaction because a second excited (S_2)-PICT state is responsible for $S_2 \rightarrow S_1$ (TICT or LE states) ultrafast internal conversion via conical intersection.[43] They emphasized the existence of a PICT minimum for planarized molecules such as NTC6, although a recent work by Hättig et al.[44] indicated that the ICT reaction of the planarized NTC6 proceeds along the twisting coordinate because of the flexibility of the amino group to some extent. Several theoretical results also emphasized the existence of the PICT state despite the energetically favorable TICT state.[20,45]

In most experiments, the ICT rate was inferred from the time profile at single wavelength for the LE or ICT bands. In addition, it was implied in the work by Pigliucci et al.[35] that the TRF of ICT state should be measured at the far red side of the emission maximum (>500 nm) because the fluorescence of the LE state extends to 500 nm.[46] In general, molecular structure of a charge separated state is strongly correlated to the solvent polarities, and therefore, the ICT rate should be affected by the solvent reorganization process. In some cases, ICT reaction rate is limited by the solvent fluctuation. Since the solvation dynamics in polar solvents usually occurs in a few picoseconds, which is similar to the ICT rate, and it manifests in the dynamic Stokes shift of the emission band, ICT dynamics and solvation process cannot be discriminated clearly in time-resolved spectroscopies. Vibrational and vibronic relaxations occur in a similar time scale as well and may obscure the ICT dynamics.

TRF is an ideal method to study the dynamics occurring in an electronic excited state, as it has a unique advantage over TA; TRF probes the electronic excited state exclusively, whereas TA is sensitive to the ground state bleach, stimulated emission, excited state absorption from both reactant and product, and ground state product absorption. TRF of DMABN will be very informative for the investigation of the ICT dynamics since both the reactant and product emit strongly. In this work, we report highly time-resolved fluorescence of DMABN at several different wavelengths to examine the ICT dynamics. TRF spectra (TRFS), in particular, measured directly over the full spectral region of interest without the conventional spectral reconstruction method allows the discrimination of the ICT dynamics from the other processes such as solvation dynamics, vibronic relaxation, and intramolecular vibrational redistribution (IVR) that cause the spectral relaxation. The ICT dynamics of DMABN in acetonitrile is determined to be much faster than the values reported previously and quite dispersive, that is, the dynamics is heterogeneous and cannot be described by a single time constant.

2. EXPERIMENTAL SECTION

2.1. Materials. DMABN and acetonitrile were purchased from Sigma-Aldrich Co. Ltd. with the highest available purity and spectrophotometric grade and used without further purifications. All measurements were made at ambient temperature (25 ± 1 °C) except otherwise noted.

2.2. Femtosecond Light Source. The femtosecond light source was based on a home-built cavity-dumped Ti:sapphire oscillator pumped by a frequency doubled Nd:YVO4 laser (Verdi, Coherent Inc.). Center wavelength and pulse duration of the fundamental output were 830 nm and 20 fs, respectively. Cavity-dumping provided 50 nJ pulse energy at the repetition rate of 380 kHz. To produce the ultrashort pump pulses at 276 nm, we first generated the second harmonic in a thin 100 μm path length lithium triborate (LBO) crystal, while preserving the pulse duration. Then, we employed sum frequency generation (SFG) of the fundamental and the second harmonic in a 300 μm thick beta-barium borate (BBO) crystal arranged in a noncollinear phase matching geometry to minimize the group velocity mismatch (GVM), which is the major source of lengthening of the pulse duration.[47,48] The remaining fundamental pulse served as the gate in the fluorescence upconversion experiment. Pulse energy of about 1 nJ was obtained at 276 nm, which was further reduced to 200 pJ to prevent any photo damage of the sample.

2.3. Femtosecond Time-Resolved Fluorescence Measurements. Femtosecond TRF was measured by fluorescence upconversion method utilizing noncollinear SFG described in detail elsewhere.[48] SFG of the fluorescence and the gate pulse was performed by using a 300 μm thick BBO crystal mounted on a motorized rotation stage. The instrument response function (IRF) estimated from the difference frequency generation (DFG) of the scattered pump pulses at 276 nm and the gate was around 110 fs fwhm (full width at half-maximum). In the actual upconversion experiments, where the fluorescence wavelength is much longer than that of the pump pulse, the time-resolution was estimated to be ∼85 fs from the numerical simulation because of the smaller GVM between the fluorescence and the gate pulse. TRFS were obtained by rotating the BBO crystal to the proper phase matching angle, while scanning the detection wavelength. All TRF measurements were performed with using magic angle. A detailed illustration of the TRFS setup is shown in Figure S1, Supporting Information. Intensities of the TRFS spectra were calibrated by using two dyes, 2-(4-biphenylyl)-5-phenyl-1,3,4-oxadizol (PBD) and coumarin 47, as references. Fluorescence spectra of the reference dyes at steady-state were compared with those at 500 ps, where solvation and vibronic relaxation processes are complete. Also, we have considered the time-zero shifts of each wavelength in a broad fluorescence due to the group velocity dispersion (GVD) appearing when the fluorescence transmits through one side of a sample cuvette (∼1.25 mm quartz). Compensation of the time-zero difference was achieved by moving the delay stage of the gate pulse considering the effective material length of each wavelength. TRFS were measured in two separate wavelength regions, 332−382 nm for the LE emission and 432−562 nm for the ICT emission, due to an experimental reason; wavelength of the upconverted fluorescence at 415 nm by the gate pulse at 830 nm coincides with the wavelength of the pump pulses at 276 nm causing excessive noise from the pump scattering. To avoid effects of an unwanted photoproduct, 4-methylaminobenzonitrile,[49] steady-state absorption and fluorescence were checked before and after measuring TRF.

3. RESULTS

3.1. Time-Resolved Fluorescence. TRF at several different wavelengths ranging from the LE to ICT emission bands is shown in Figure 1. The TRFs measured at 330 and 350 nm represent mostly the emission from the LE state, whereas the TRFs at 500 and 600 nm represent the emission from the ICT state almost exclusively. Each time trace was nonlinear-least-squares fitted to a sum of exponential functions, and the results are summarized in Table 1. The time constant of the slowest decay component was fixed to ∼3 ns, determined from the picosecond TRF measured by time-correlated single

dx.doi.org/10.1021/jp310842z | J. Phys. Chem. A 2013, 117, 370−377

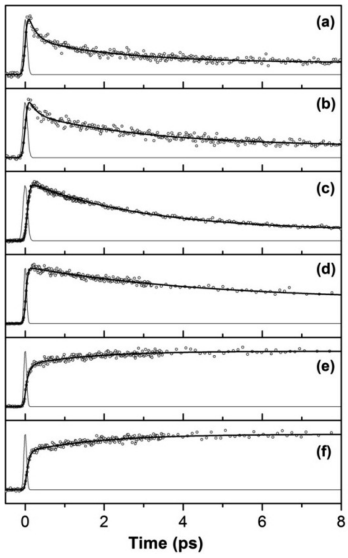

Figure 1. Time-resolved fluorescence (TRF) of DMABN in acetonitrile detected at (a) 330, (b) 350, (c) 380, (d) 450, (e) 500, and (f) 600 nm. Instrument response is also shown.

Table 1. Exponential Fit Results for the Femtosecond TRFs Detected at the Given Wavelengths; Numbers in Parentheses Are the Relative Amplitudes within the Rise or Decay; Negative Amplitudes Represent Rise Components

330 nm	350 nm	380 nm	450 nm	500 nm	600 nm
180 fs (50%)	190 fs (34%)	<30 fs (−100%)	<30 fs (−70%)	<30 fs (−60%)	<30 fs (−40%)
			130 fs (−30%)	200 fs (−20%)	110 fs (−20%)
2.7 ps (35%)	2.9 ps (50%)	3.0 ps (85%)	2.4 ps (34%)	2.5 ps (−20%)	2.6 ps (−40%)
3 ns (15%)	3 ns (16%)	3 ns (15%)	3 ns (66%)	3 ns (100%)	3 ns (100%)

photon counting (TCSPC) method. The TRF signals are characterized by decays or rises that consist of nearly instantaneous (<30 fs), 100−200 fs, and ∼2.7 ps. These ultrafast decays and rises within a few hundred femtoseconds were either unidentified or largely ignored because the femtosecond decays or rises were believed to be originated from the fast solvation dynamics of acetonitrile,[25] which is nearly complete within 1 ps,[50] and the emissions in 380−450 nm were considered as a mixed fluorescence from both ICT and LE states.[51]

Meanwhile, the highlight of the TRF is that a nearly instantaneous rise (<30 fs) component is clearly observed at all wavelengths of the ICT emission band even at 600 nm (Figure S2, Supporting Information compares the TRF time profiles at 500, 550, and 600 nm). This near instantaneous rise of the ICT emission was not recognized in previous reports, except the one by Rettig and co-workers, where an instrument-limited ultrafast rise at 500 nm was noted.[35] Interference from the red tail of the LE state emission was invoked as the origin of the instantaneous rise.[46] However, the LE emission band does not extend over 500 nm in nonpolar solvent, where ICT does not occur. In addition, a picosecond TRFS also does not show the long red tail in the LE emission band.[51] In our femtosecond TRF experiment, the near instantaneous rise is still prominent even at the very reddish 600 nm, which confirms the presence of the nearly instantaneous rise of the ICT emission.

These seemingly inconsistent dynamics observed in the TRF is a result of the spectral dynamics of both LE and ICT emissions convoluted with the ICT dynamics. Moreover, the ICT reaction dynamics itself could be dispersive in nature, that is, the dynamics may be characterized by many (even continuous) time constants arising from the conformational distribution of the DMABN in the ground state. Therefore, separation of the ICT dynamics from other processes that cause spectral dynamics, such as solvation, vibronic relaxation, and IVR, is crucial. The separation can be best achieved by the TRFS measurements followed by the integrated intensity analysis.

3.2. Time-Resolved Fluorescence Spectra on LE State.

Figure 2a shows the TRFS of the LE state at several time delays measured directly by the fluorescence upconversion method without the conventional spectral reconstruction. The LE emission spectrum is centered at around 350 nm and rises instantaneously to reach the maximum intensity at 100 fs. Under the Condon approximation, the integrated intensity of TRFS represents the population of the LE state. The decrease of the integrated intensity is biphasic displaying initial ultrafast decay followed by slower decay of a few picosecond time scale. Interestingly, the TRFS of the LE state exhibits the spectral dynamics as well; the TRFS red-shifts as time increases. Such dynamic Stokes shift can be attributed to the solvation dynamics of the LE state in acetonitrile. Each TRF spectrum was fitted to a log-normal function to estimate center frequency and integrated intensity. The center frequency vs time shown in Figure 2b can be well represented by a biexponential function with time constants of 110 and 340 fs. The solvation dynamics of acetonitrile is known to proceed by two time constants of 89 and 630 fs, where the femtosecond component is the major

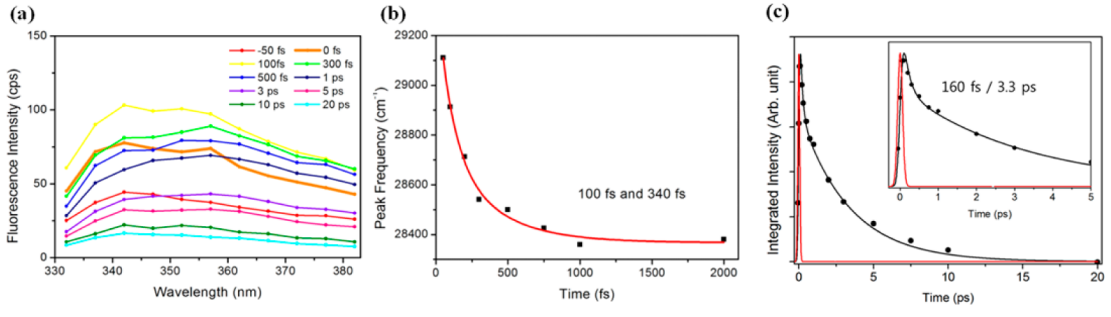

Figure 2. (a) TRFS on LE state, (b) peak frequency, and (c) integrated intensity profiles on the TRFS. The peak frequency is fitted by two time constants of 100 and 340 fs and the intensity profile is fitted by two time constants of 160 fs, 3.3 ps, and a much longer time constant (not shown).

dx.doi.org/10.1021/jp310842z | J. Phys. Chem. A 2013, 117, 370−377

component comprising nearly 70% of the total solvation.[50] Correspondence of the time constants corroborates the assignment of the dynamics Stokes shift of the LE band to the solvation dynamics, although shortening of the longer time constant from 630 to 340 fs may indicate that vibronic relaxation and IVR may play roles.

The integrated intensity of TRFS in Figure 2c represents the population dynamics of the LE state, which can be fitted well by a three-exponential function with time constants of 160 fs, 3.3 ps, and a much longer time. They are similar to the time constants from the TRF of the LE emission at 330 nm. The two fast time constants can be assigned to the ICT reaction unambiguously, as they are also observed in the rise of the ICT emission (vide infra). Therefore, the femtosecond TRFS of the LE state clearly shows that the ICT dynamics of DMABN is dispersive ranging from nearly instantaneous to several picoseconds, and the ICT dynamics for the most part occurs much faster than the previously reported value of ~4 ps.[25,35,36]

3.3. Time-Resolved Fluorescence Spectra on ICT State. Figure 3 shows the TRFS measured in the ICT emission region. At the wavelengths longer than 500 nm, it is remarkable to find again the instrument limited rise of the ICT emission and the ICT band continues to grow up to a few picoseconds as observed in the single wavelength measurements in Figure 1 (Table 1). In addition, growth of an additional band at around 450 nm is also obvious. This feature grows up to ~300 fs at a rate similar to the faster time constant (160 fs) in the decay of the integrated intensity of the LE state and then undergoes a decay as well as dynamic Stokes shift. The decay time constant of the 450 nm feature matches roughly with the rise time constants at 500 and 600 nm, which indicates that the 450 nm feature undergoes a relaxation process toward the more stable ICT state observed at longer wavelengths. The 450 nm feature was not observed in the steady-state fluorescence or in the picosecond TRF[51] probably due to its fast rise and decay dynamics. Interestingly, its wavelength matches with the fluorescence maxima of NTC6 in acetonitrile,[30,31] which is a planarized analogue of DMABN. Note that NTC6 is still flexible enough to have a partially twisted conformation in the ICT state that emits at 440 nm.[44] The integrated intensity for λ > 500 nm shown in Figure 3c, which may correspond to the fully relaxed ICT state (vide infra), shows the ultrafast and 2.7 ps rise components.

To investigate the spectral dynamics of the ICT band, the TRFS were normalized as shown in Figure 4a. The center frequency of the ICT band redshifts continuously up to 30 ps to reach the center frequency (480 nm) of the steady-state fluorescence spectrum. The center frequency, shown in Figure 4b, can be fitted well to an exponential function with time constants of 4.8 ps. Note that the dynamic Stokes shift for a probe molecule (coumarin 153) in acetonitrile, which includes both the solvation dynamics and vibronic relaxation, is complete at ~1 ps.[50] It is important to note that, when the relaxation in the solvent coordinate and the intensity rise dynamics of the >480 nm feature are completed at ~5 ps, the TRFS is still centered at ~455 nm, which is much shorter than the wavelength of the steady-state emission maximum. The dynamic Stokes shift far beyond the solvation time scale is a strong indication that it may not be solely due to the solvation process, and it could be originated from the relaxation of the intramolecular nuclear coordinate such as the rotation of the dimethylamino group toward the low lying TICT state.

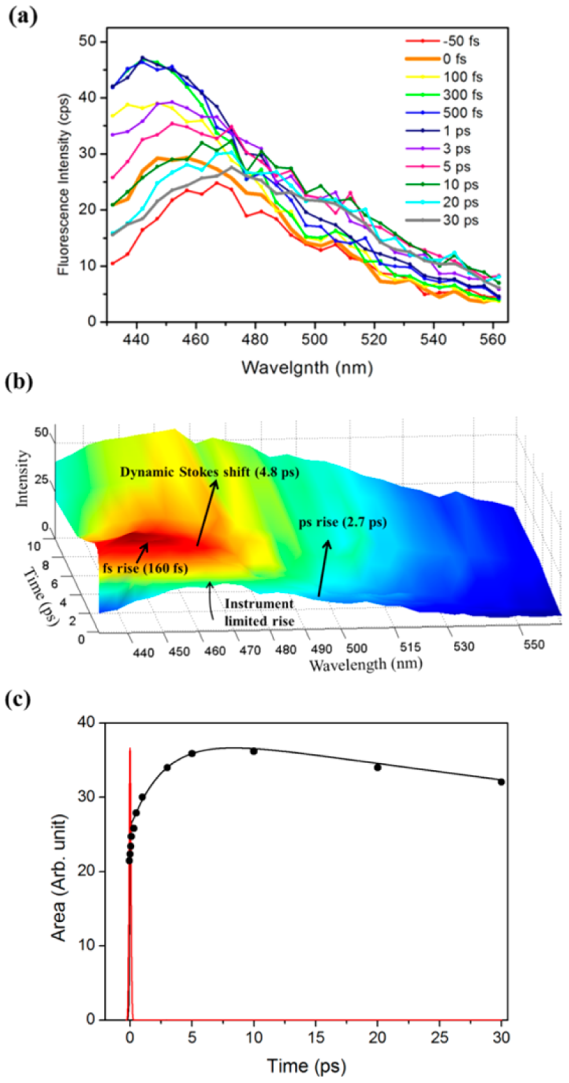

Figure 3. Time-resolved fluorescence spectra (TRFS) of DMABN in acetonitrile at the ICT emission region; (a) TRFS and (b) 3-dimensional plot. The 3-dimensional plot shows instrument limited rise, fs rise (160 fs), ps rise (2.7 ps), and dynamic Stokes shift (4.8 ps). (c) Integrated intensity for the region λ > 500 nm. An instrument limited rise, 2.7 ps rise, and >150 ps decay components can be obtained.

4. DISCUSSION

We have investigated the ICT reaction dynamics of DMABN in acetonitrile in detail by employing highly time-resolved fluorescence spectra. The ICT reaction itself may be strongly coupled with the solvent, and the ICT state undergoes an extensive solvation process in polar solvents. Therefore, the ICT dynamics should be separated from the solvation dynamics of the ICT (and LE) state. In this work, the separation has been achieved by full TRF spectra measurement over the region of interest, and the ICT rate was determined from the TRFS of the LE and ICT bands. One can argue that, since the solvation of the LE state is presumed to be minimal in polar solvent because of its small dipole moment, ICT rate can be determined unambiguously from the TRF decay of the LE state. However, TRFS of the LE state revealed that solvation of the LE state is also significant, implying its polar character. The solvation of the LE state was determined to proceed by two time constants, 110 and 340 fs. Polar solvation dynamics of

dx.doi.org/10.1021/jp310842z | J. Phys. Chem. A 2013, 117, 370−377

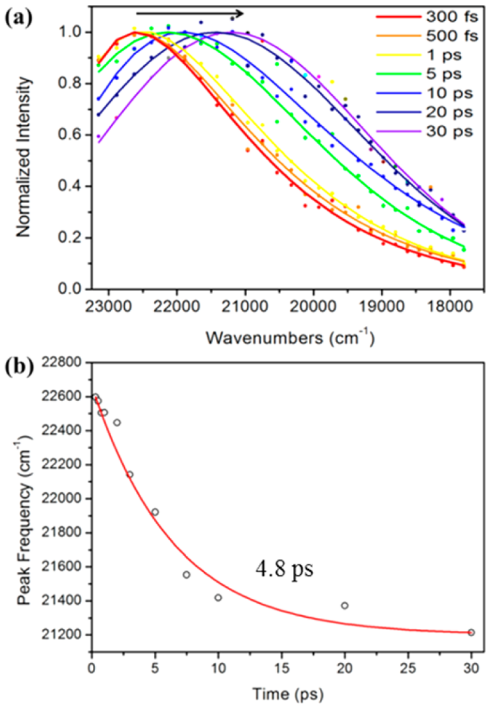

Figure 4. (a) TRFS at the ICT emission region (Figure 3) is normalized to better show the redshift of the ICT emission band indicated by the arrow. (b) Time profile of the center frequency of the ICT emission band, which can be represented by a single exponential of 4.8 ps.

acetonitrile have been studied extensively. The polar solvation dynamics of coumarin in acetonitrile proceeds by two time constants, 89 and 630 fs,[50] which is in good agreement with the time constants found in this work. Moreover, reaction dynamics derived from the time trace at a single wavelength may pose a problem because decay of the reactant population and rise of the product do not always match, especially for a system with dispersive dynamics. One prominent example is the excited state intramolecular proton transfer (ESIPT) of the polyquinoline reported previously,[52] where the decay of the reactant and the rise of the product were vastly different due to the dispersive dynamics originating from the conformational heterogeneity.

The main finding of this work can be summarized as follows. First, the ICT rate cannot be characterized by one time constant, and for the most part, it is much faster than the previous findings.[25,35,36] We found three time constants for the ICT reaction; an ultrafast component (<30 fs) limited by the instrument response, 160 fs, and 2.7 ps. The TRFS together with the fact that the instantaneous component is the major contribution even at the far red side of the ICT emission band excludes the experimental ambiguity such as interpreting its origin as the red tail of the LE band. It was also noted that the 4-(*N*,*N*-dimethylamino)-4′-cyanostilbene in polar solvent had a large amount of CT character immediately after the excitation.[53] Second, we found a transient species, the 450 nm feature, emitting on the blue side of the ICT emission band. This transient emission increases in intensity up to 300 fs, and decays by a few picosecond, while the ICT emission shows the corresponding rise. Interestingly, the transient species emits at 450 nm, where the ICT emission band of NTC6, a planarized analogue of DMABN, is observed,[30,31] while the fluorescence maximum of DMABN in acetonitrile is at 480 nm. Third, an important finding from the TRFS in the ICT emission region is that the dynamic Stokes shift of the ICT band proceeds by a 4.8 ps time constant, much longer than the dielectric relaxation of acetonitrile. We assign this process to the relaxation of the intramolecular nuclear coordinate, and this could well be the rotation of the dimethylamino group to the perpendicular position (TICT). In addition, when the usual solvation dynamics of acetonitrile and the intensity dynamics at >500 nm are completed at ∼5 ps, the ICT emission spectrum is still centered at 455 nm as shown in Figure 3a, which indicates that further relaxation is required to reach ICT steady-state fluorescence centered at 480 nm. Consequently, we can identify at least three emitting species; the LE, the partially twisted 450 nm feature called ICT(P), and the fully relaxed state called ICT(T).

The ultrafast reaction rates in femtosecond range may rule out the 90° twisted ICT as a possible mechanism because the twisting motion of the amino group with respect to the planar benzonitrile group cannot occur by a few hundred femtoseconds. Theoretical studies have established that, at room temperature, DMABN molecules on the ground state cannot exist close to the 90° twisted form of the dimethylamino group for their high energy but remains near planar at room temperature.[13,14,20−22] On the basis of the experimental findings in this work together with the previous theoretical reports, we propose a model shown in Scheme 1. It is well-known that the photoexcitation of DMABN creates ^1L_a (S_2) state. The instrument limited rises of both LE and part of ICT emissions indicate that both states are populated within 30 fs. The LE state thus created undergoes ICT reaction by two time constants, 160 fs and 3.3 ps. The former one represents dynamics to the ICT state that emits at around 450 nm (ICT(P)). The structure of the state emitting at 450 nm ICT(P) may be close to the ICT state of NTC6, i.e., twisted to some extent but not a fully twisted amino group. The ICT(P) state undergoes further intramolecular relaxation and to reach the more twisted form ICT(T) state within 4.8 ps. In addition, the 3.3 ps time constant for the decay LE state implies that there exists another channel to the ICT(T) state as suggested in previous reports.[4,35,37] Interestingly, Coto et al. suggested in theoretical and experimental studies that both fluorescent TICT and dark TICT states exist.[54] The twist angle of the dimethylamino group was calculated to be 53.4° for the fluorescent TICT state, whereas the dark TICT state is fully twisted.[54]

Scheme 1. Schematic of the Intramolecular Charge Transfer Pathways of DMABN in Acetonitrile Following the Photoexcitation by 276 nm Light

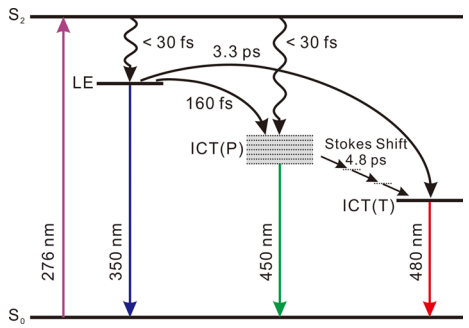

dx.doi.org/10.1021/jp310842z | J. Phys. Chem. A 2013, 117, 370−377

Here, we should emphasize that the initial charge transfer reaction to ICT(P) is complete within a few hundred femtoseconds and that the subsequent further twisting is the relaxation of the intramolecular nuclear coordinate within the ICT state. TRFS also indicates that part of the emission at around 450 nm appears immediately (<30 fs) after the excitation, which requires the channel that populates ICT(P) and part of ICT(T) directly from the initial excited state. Considering distribution of the rotation angle of the dimethylamino group in the ground state, the structure of the ICT(P) state is probably twisted by a small amount because the fully twisted geometry is energetically unfavorable in the ground state.

There have been some discussions about the nature of the initial excited state, that is, the LE state (not ^1L_a) is populated by the initial photoexcitation.[55,56] However, even the current experiments cannot differentiate the possibility of the initial direct excitation to the LE and ICT(P) state from the ground state. In this case, the above scheme should be modified slightly; initial photoexcitation creates both LE and ICT(P). However, considering the large energy difference between the initial photoexcited state and ICT(P), it is unlikely that the initial photoexcitation creates both LE and ICT(P) states.

Our model summarized in Scheme 1 proposes dispersive ICT dynamics for DMABN; instrument limited rise of ICT(P), further relaxation to ICT(T), and the LE contribution (3.3 ps) to ICT(T). Interestingly, initial ultrafast dynamics in our scheme is consistent with the theoretical calculation by Robb and co-workers:[43] they reported that, after the initial excitation to the S_2 state, the system quickly reaches the S_2-(P)ICT minimum. Subsequently, ultrafast nonradiative S_2/S_1 decay takes place at various torsion angles of the dimethyl-amino group leading to either S_1-LE or S_1-(T)ICT geometries because of the extended conical intersection seam.

Interestingly, some of the time-resolved vibrational spectroscopies support the TICT model unequivocally.[15,57] That is, at picosecond time resolution, the molecule has a TICT structure. Notably, the work by Kwok et al.[10] showed unambiguously that the ICT state is in the TICT geometry by detailed time-resolved resonance Raman studies on several isotopes and the ph-N vibrational frequency of the ICT state. These findings, however, can be incorporated straightforwardly within our proposed reaction mechanism. Time-resolved vibrational spectroscopies require picosecond time resolution to maintain the frequency resolution. In fact, the Raman spectra were recorded at 50 ps after the excitation. Therefore, the Raman spectra should probe the excited state after the completion of the intramolecular relaxation, which should be the TICT state.

The multifaceted ICT reaction dynamics of DMABN including the nearly instantaneous component can be accounted for by invoking conformation-dependent reaction rates and pathways. The potential energy surface of the ground state along the twisting coordinate of the amino group is rather shallow to allow a distribution of the torsion angle in the ground state.[4] So a molecule whose conformation in the ground is close to that of the ICT state may undergo ultrafast ICT, whereas a molecule whose conformation is distant from that of the ICT state may undergo slower ICT reaction via LE state, which involves the twisting motion of the amino group. In this view, the biexponential behavior (160 fs and 3.3 ps) of the LE to ICT can also be accounted for by the distribution of the reaction rates on the initial (ground state) conformation of the molecules. Kim et al. showed that the ICT dynamics of Laurdan, an analogue of DMABN, also exhibits dispersive dynamics including an instantaneous component by the TRFS and the observation of the coherent nuclear wave packet on the product ICT state.[58] The possibility of a faster ICT reaction rate for a certain geometry in a pretwisted structure was noted, assuming that the potential energy surface (PES) is barrierless, such as the PES of nonadiabatic coupling between S_2 and S_1.[59,60]

The picosecond component of the ICT rate is strongly solvent dependent,[61] which implies that this part of ICT reaction may be driven by the solvent fluctuation as observed for some electron transfer reactions in the context of the Sumi/Marcus model,[59,62,63] where an electron transfer rate is proportional to solvent reorganization. The solvent-driven ICT reaction mechanism[64,65] can also be incorporated within the context of the conformational heterogeneity model; a molecule whose conformation is distant from that of the ICT state may undergo slower ICT reaction through the twisting of the amino group aided by the solvent fluctuation. It is also supported by the Kim and Hynes (KH) model, which is based on the two-dimensional dynamics of solvation and twist coordinates including the frictional damping of solvents and calculates the activation free energy ($\Delta G^{\ddagger}$) of various solvents, the calculated barrier energy of 1.5 kcal/mol (~6 kJ/mol) was obtained,[41] which is consistent with our result in Figures S3 and S4 and Table S1, Supporting Information.

5. CONCLUSIONS

In this work, we have investigated the ICT reaction dynamics of DMABN in acetonitrile by employing highly time-resolved fluorescence spectra. In particular, the ICT dynamics was measured independent of the solvation dynamics of the ICT and LE states and vibronic relaxation by means of the TRF spectra measurement over the full wavelength region of interest. The most important finding of this work is that, in contrast to the numerous previous reports, the ICT dynamics cannot be characterized by a single time constant. Rather, the dynamics can be represented by a broad range of time scales. Therefore, it cannot be explained by a simple two-state model such as the population transfer between the LE and ICT states. TRF and TRFS identified at least three states emitting at 350, 450, and 480 nm, which were assigned to LE, ICT(P), and ICT(T), respectively. Therefore, it cannot be explained by a simple two-state model such as the population transfer between the LE and ICT states. In addition, within a few hundred femtoseconds after the photoexcitation, an ICT(P) state that has a small twist angle is formed from the LE state and directly from S_2. ICT(P) undergoes further relaxation along the intramolecular nuclear coordinate, which could well be the rotation of the dimethylamino group, to reach the ICT(T) state by the 4.8 ps time constant. There is also an additional channel from the LE to ICT(T) state.

To account for this multifaceted reaction dynamics, we propose a conformational heterogeneity of DMABN in the ground state along the rotational coordinate of the dimethylamino group; reaction rates and pathways could be distinct depending on the twist angle of the dimethylamino group in the ground state.

■ ASSOCIATED CONTENT

Supporting Information

Detailed illustration of the TRFS setup, comparison of instantaneous rises shown on TRFs at 500, 550, and 600 nm,

dx.doi.org/10.1021/jp310842z | J. Phys. Chem. A 2013, 117, 370−377

and temperature-dependent TRF measured at 7, 25, and 45 °C. This material is available free of charge via the Internet at http://pubs.acs.org.

AUTHOR INFORMATION

Corresponding Author

*Tel: +82-54-279-2122. Fax: +82-54-279-8127. E-mail: thjoo@postech.ac.kr.

Notes

The authors declare no competing financial interest.

ACKNOWLEDGMENTS

This work was supported by the National Research Foundation of Korea (NRF) grant funded by the Korea government (MEST) (2007-0056330) and the Global Research Laboratory Program (2009-00439).

REFERENCES

(1) Lippert, E.; Ludar, W.; Boss, H. *Advances in Molecular Spectroscopy*; Pergamon Press: Oxford, U.K., 1962.
(2) Rotkiewicz, K.; Grellmann, K. H.; Grabowski, Z. R. *Chem. Phys. Lett.* **1973**, *19*, 315−318.
(3) Rettig, W. *Angew. Chem., Int. Ed.* **1986**, *25*, 971−988.
(4) Grabowski, Z. R.; Rotkiewicz, K.; Rettig, W. *Chem. Rev.* **2003**, *103*, 3899−4031.
(5) Parasassi, T.; Krasnowska, E. K.; Bagatolli, L.; Gratton, E. *J. Fluoresc.* **1998**, *8*, 365−373.
(6) Kim, H. M.; Jeong, B. H.; Hyon, J. Y.; An, M. J.; Seo, M. S.; Hong, J. H.; Lee, K. J.; Kim, C. H.; Joo, T. H.; Hong, S. C.; Cho, B. R. *J. Am. Chem. Soc.* **2008**, *130*, 4246−4247.
(7) Kajimoto, O.; Yokoyama, H.; Ooshima, Y.; Endo, Y. *Chem. Phys. Lett.* **1991**, *179*, 455−459.
(8) Hashimoto, M.; Hamaguchi, H. *J. Phys. Chem.* **1995**, *99*, 7875−7877.
(9) Chudoba, C.; Kummrow, A.; Dreyer, J.; Stenger, J.; Nibbering, E. T. J.; Elsaesser, T.; Zachariasse, K. A. *Chem. Phys. Lett.* **1999**, *309*, 357−363.
(10) Kwok, W. M.; Ma, C.; Matousek, P.; Parker, A. W.; Phillips, D.; Toner, W. T.; Towrie, M. *Chem. Phys. Lett.* **2000**, *322*, 395−400.
(11) Kwok, W. M.; Ma, C.; Phillips, D.; Matousek, P.; Parker, A. W.; Towrie, M. *J. Phys. Chem. A* **2000**, *104*, 4188−4197.
(12) Okamoto, H.; Inishi, H.; Nakamura, Y.; Kohtani, S.; Nakagaki, R. *Chem. Phys.* **2000**, *260*, 193−214.
(13) Cammi, R.; Mennucci, B.; Tomasi, J. *J. Phys. Chem. A* **2000**, *104*, 5631−5637.
(14) Mennucci, B.; Toniolo, A.; Tomasi, J. *J. Am. Chem. Soc.* **2000**, *122*, 10621−10630.
(15) Kwok, W. M.; Ma, C.; Matousek, P.; Parker, A. W.; Phillips, D.; Toner, W. T.; Towrie, M.; Umapathy, S. *J. Phys. Chem. A* **2001**, *105*, 984−990.
(16) Ma, C.; Kwok, W. M.; Matousek, P.; Parker, A. W.; Phillips, D.; Toner, W. T.; Towrie, M. *J. Phys. Chem. A* **2002**, *106*, 3294−3305.
(17) Fuβ, W.; Pushpa, K. K.; Rettig, W.; Schmid, W. E.; Trushin, S. A. *Photochem. Photobiol. Sci.* **2002**, *1*, 255−262.
(18) Towrie, M.; Grills, D. C.; Dyer, J.; Weinstein, J. A.; Matousek, P.; Barton, R.; Bailey, P. D.; Subramaniam, N.; Kwok, W. M.; Ma, C. S.; Phillips, D.; Parker, A. W.; George, M. W. *Appl. Spectrosc.* **2003**, *57*, 367−380.
(19) Köhn, A.; Hättig, C. *J. Am. Chem. Soc.* **2004**, *126*, 7399−7410.
(20) Cogan, S.; Zilberg, S.; Haas, Y. *J. Am. Chem. Soc.* **2006**, *128*, 3335−3345.
(21) Chiba, M.; Tsuneda, T.; Hirao, K. *J. Chem. Phys.* **2007**, *126*, 11.
(22) Carlotto, S.; Polimeno, A.; Ferrante, C.; Benzi, C.; Barone, V. *J. Phys. Chem. B* **2008**, *112*, 8106−8113.
(23) Scholes, G. D.; Phillips, D.; Gould, I. R. *Chem. Phys. Lett.* **1997**, *266*, 521−526.
(24) Yoshihara, T.; Druzhinin, S. I.; Zachariasse, K. A. *J. Am. Chem. Soc.* **2004**, *126*, 8535−8539.
(25) Druzhinin, S. I.; Ernsting, N. P.; Kovalenko, S. A.; Lustres, L. W.; Senyushkina, T. A.; Zachariasse, K. A. *J. Phys. Chem. A* **2006**, *110*, 2955−2969.
(26) Schuddeboom, W.; Jonker, S. A.; Warman, J. M.; Leinhos, U.; Kuehnle, W.; Zachariasse, K. A. *J. Phys. Chem.* **1992**, *96*, 10809−10819.
(27) Gorse, A.-D.; Pesquer, M. *J. Phys. Chem.* **1995**, *99*, 4039−4049.
(28) Sobolewski, A. L.; Domcke, W. *Chem. Phys. Lett.* **1996**, *250*, 428−436.
(29) Sobolewski, A. L.; Sudholt, W.; Domcke, W. *J. Phys. Chem. A* **1998**, *102*, 2716−2722.
(30) Druzhinin, S. I.; Kovalenko, S. A.; Senyushkina, T.; Zachariasse, K. A. *J. Phys. Chem. A* **2007**, *111*, 12878−12890.
(31) Zachariasse, K. A.; Druzhinin, S. I.; Bosch, W.; Machinek, R. *J. Am. Chem. Soc.* **2004**, *126*, 1705−1715.
(32) Zachariasse, K. A.; Druzhinin, S. I.; Mayer, P.; Kovalenko, S. A.; Senyushkina, T. *Chem. Phys. Lett.* **2009**, *484*, 28−32.
(33) Zachariasse, K. A.; Druzhinin, S. I.; Kovalenko, S. A.; Senyushkina, T. *J. Chem. Phys.* **2009**, *131*, 224313.
(34) Techert, S.; Zachariasse, K. A. *J. Am. Chem. Soc.* **2004**, *126*, 5593−5600.
(35) Pigliucci, A.; Vauthey, E.; Rettig, W. *Chem. Phys. Lett.* **2009**, *469*, 115−120.
(36) Fujiwara, T.; Zgierski, M. Z.; Lim, E. C. *Phys. Chem. Chem. Phys.* **2011**, *13*, 6779−6783.
(37) Gustavsson, T.; Coto, P. B.; Serrano-Andres, L.; Fujiwara, T.; Lim, E. C. *J. Chem. Phys.* **2009**, *131*, 031101.
(38) Polimeno, A.; Barbon, A.; Nordio, P. L.; Rettig, W. *J. Phys. Chem.* **1994**, *98*, 12158−12168.
(39) Hayashi, S.; Ando, K.; Kato, S. *J. Phys. Chem.* **1995**, *99*, 955−964.
(40) Serranoandres, L.; Merchan, M.; Roos, B. O.; Lindh, R. *J. Am. Chem. Soc.* **1995**, *117*, 3189−3204.
(41) Kim, H. J.; Hynes, J. T. *J. Photochem. Photobiol., A* **1997**, *105*, 337−343.
(42) Rappoport, D.; Furche, F. *J. Am. Chem. Soc.* **2004**, *126*, 1277−1284.
(43) Gómez, I.; Reguero, M.; Boggio-Pasqua, M.; Robb, M. A. *J. Am. Chem. Soc.* **2005**, *127*, 7119−7129.
(44) Hättig, C.; Hellweg, A.; Köhn, A. *J. Am. Chem. Soc.* **2006**, *128*, 15672−15682.
(45) Dreyer, J.; Kummrow, A. *J. Am. Chem. Soc.* **2000**, *122*, 2577−2585.
(46) Rettig, W.; Bliss, B.; Dirnberger, K. *Chem. Phys. Lett.* **1999**, *305*, 8−14.
(47) Radzewicz, C.; Band, Y. B.; Pearson, G. W.; Krasinski, J. S. *Opt. Commun.* **1995**, *117*, 295−302.
(48) Rhee, H.; Joo, T. *Opt. Lett.* **2005**, *30*, 96−98.
(49) Druzhinin, S. I.; Galievsky, V. A.; Zachariasse, K. A. *J. Phys. Chem. A* **2005**, *109*, 11213−11223.
(50) Horng, M. L.; Gardecki, J. A.; Papazyan, A.; Maroncelli, M. *J. Phys. Chem.* **1995**, *99*, 17311−17337.
(51) Koti, A. S. R.; Periasamy, N. *Res. Chem. Intermed.* **2002**, *28*, 831−836.
(52) Kim, C. H.; Chang, D. W.; Kim, S.; Park, S. Y.; Joo, T. *Chem. Phys. Lett.* **2008**, *450*, 302−307.
(53) Eilers-König, N.; Kühne, T.; Schwarzer, D.; Vöhringer, P.; Schroeder, J. *Chem. Phys. Lett.* **1996**, *253*, 69−76.
(54) Coto, P. B.; Serrano-Andres, L.; Gustavsson, T.; Fujiwara, T.; Lim, E. C. *Phys. Chem. Chem. Phys.* **2011**, *13*, 15182−15188.
(55) Fujiwara, T.; Lee, J. K.; Zgierski, M. Z.; Lim, E. C. *Chem. Phys. Lett.* **2009**, *481*, 78−82.
(56) Galievsky, V. A.; Druzhinin, S. I.; Demeter, A.; Mayer, P.; Kovalenko, S. A.; Senyushkina, T. A.; Zachariasse, K. A. *J. Phys. Chem. A* **2010**, *114*, 12622−12638.
(57) Okamoto, H.; Inishi, H.; Nakamura, Y.; Kohtani, S.; Nakagaki, R. *J. Phys. Chem. A* **2001**, *105*, 4182−4188.

(58) Kim, S. Y.; Kim, C. H.; Park, M.; Ko, K. C.; Lee, J. Y.; Joo, T. *J. Phys. Chem. Lett.* **2012**, *3*, 2761−2766.
(59) Bagchi, B.; Fleming, G. R. *J. Phys. Chem.* **1990**, *94*, 9−20.
(60) Bagchi, B. *Chem. Phys. Lett.* **1987**, *135*, 558−564.
(61) Changenet, P.; Plaza, P.; Martin, M. M.; Meyer, Y. H. *J. Phys. Chem. A* **1997**, *101*, 8186−8194.
(62) Sumi, H.; Marcus, R. A. *J. Chem. Phys.* **1986**, *84*, 4894−4914.
(63) Liu, M.; Ito, N.; Maroncelli, M.; Waldeck, D. H.; Oliver, A. M.; Paddon-Row, M. N. *J. Am. Chem. Soc.* **2005**, *127*, 17867−17876.
(64) Walker, G. C.; Aakesson, E.; Johnson, A. E.; Levinger, N. E.; Barbara, P. F. *J. Phys. Chem.* **1992**, *96*, 3728−3736.
(65) Barbara, P. F.; Walker, G. C.; Smith, T. P. *Science* **1992**, *256*, 975−981.